

This article was downloaded by:

On: 25 January 2011

Access details: *Access Details: Free Access*

Publisher *Taylor & Francis*

Informa Ltd Registered in England and Wales Registered Number: 1072954 Registered office: Mortimer House, 37-41 Mortimer Street, London W1T 3JH, UK



Separation Science and Technology

Publication details, including instructions for authors and subscription information:

<http://www.informaworld.com/smpp/title~content=t713708471>

Experimental Study of the Effect of Membrane Porosity on Membrane Absorption Process

Zeting Zhang^a; Jian Gao^a; Weidong Zhang^a; Zhongqi Ren^a

^a The Ministry of Education Key Laboratory of Science and Technology of Controllable Chemical Reactions, Beijing University of Chemical Technology, Beijing, PR China

To cite this Article Zhang, Zeting , Gao, Jian , Zhang, Weidong and Ren, Zhongqi(2006) 'Experimental Study of the Effect of Membrane Porosity on Membrane Absorption Process', *Separation Science and Technology*, 41: 14, 3245 – 3263

To link to this Article: DOI: 10.1080/01496390600851707

URL: <http://dx.doi.org/10.1080/01496390600851707>

PLEASE SCROLL DOWN FOR ARTICLE

Full terms and conditions of use: <http://www.informaworld.com/terms-and-conditions-of-access.pdf>

This article may be used for research, teaching and private study purposes. Any substantial or systematic reproduction, re-distribution, re-selling, loan or sub-licensing, systematic supply or distribution in any form to anyone is expressly forbidden.

The publisher does not give any warranty express or implied or make any representation that the contents will be complete or accurate or up to date. The accuracy of any instructions, formulae and drug doses should be independently verified with primary sources. The publisher shall not be liable for any loss, actions, claims, proceedings, demand or costs or damages whatsoever or howsoever caused arising directly or indirectly in connection with or arising out of the use of this material.

Experimental Study of the Effect of Membrane Porosity on Membrane Absorption Process

Zeting Zhang, Jian Gao, Weidong Zhang, and Zhongqi Ren

The Ministry of Education Key Laboratory of Science and Technology of
Controllable Chemical Reactions, Beijing University of Chemical
Technology, Beijing, PR China

Abstract: Five kinds of expanded polytetrafluoroethylene (ePTFE) flat membranes with different porosity and micro-pore size were chosen to carry out the unsteady state gas absorption experiments. The influence of the membrane porosity and micro-pore size on the membrane absorption process was investigated. Experimental results showed that the membrane porosity had an impact on the membrane absorption process, and the degree of this impact depended on the absorption system and the membrane pore size. For a rapid mass transfer process, the porosity affected the mass transfer more significantly, while for the slow mass transfer process the porosity almost did not affect the mass transfer. The modeling analysis showed that the porosity affected the concentration profile of the solute near the membrane surface on the liquid side, which led to the reduction of the mass transfer area of the membrane. Hence, the apparent effect on the mass transfer of the membrane absorption process.

Keywords: Membrane absorption, mass transfer process, membrane porosity

INTRODUCTION

Gas membrane absorption was first proposed for a blood oxygenator in 1975 (1). In the membrane absorption process, the membrane provides a steady

Received 20 January 2005, Accepted 1 June 2006

Address correspondence to Weidong Zhang, The Ministry of Education Key Laboratory of Science and Technology of Controllable Chemical Reactions, College of Chemical Engineering, Beijing University of Chemical Technology, PO Box 1#, Beijing 100029, PR China. Tel.: +86-010-6443-4788; E-mail: zhangwd@mail.buct.edu.cn

interface between the gas and the liquid phases, and compared to the traditional absorption towers (2), it prevents problems like flooding, unloading, channeling, lower efficiency, etc., Zhang Qi and Cussler (3) were the first to demonstrate the use of the hollow fiber membrane contactor for gas cleanup in 1985, and since then, many researchers have done a lot of studies in terms of mass transfer mechanism, non-ideal fluid dynamics on the shell side, and its application (1–5).

In many of these studies of the membrane absorption process, the *resistance-in-series* model has been used to describe the mass transfer process, and the calculations of mass transfer resistances on the tube side, the shell side, and in the membrane phase have brought about many correlations. Most of these reports (3, 4, 7–9) have presented similar correlations of the mass transfer resistances on the tube side and the membrane phase, whereas correlations of the shell side mass transfer are quite different in each study (3, 4, 7–9). Many researchers (4, 7–9) attributed this difference to a non-ideal flow and end-effects on the shell side. However, it has been found that some of these mass transfer correlations were based on the total area of the pores (10, 11), while the others were based on the whole membrane area (12, 13). This may be one of the reasons that have brought about the different correlations of the shell side mass transfer in the hollow fiber membrane absorption process. The membrane porosity is the key factor that affects the mass transfer area in the membrane absorption process. However, it is regretful to note that most researchers believe that the porosity only changes the mass transfer resistance of the membrane phase (3, 4, 7–9). Kim et al. (10) and Baudot et al. (11) pointed out that the mass transfer process should take place through the micro pores only, and that the contact area should be the total area of the pores, implying that the membrane porosity could significantly affect the mass transfer. However, Karoor et al. (12) and Kreulen et al. (13) believed that the whole membrane area should be used to calculate the mass transfer coefficient, and they found that the membrane porosity had no effect on the mass transfer process, according to their calculation. These two kinds of viewpoints are quite conflicting. According to the analysis of mass transfer behavior near the membrane surface in the membrane absorption process, the solute mass transfer on the membrane surface on the liquid side has two directions. One is in the vertical (normal) direction, the other is along the membrane surface (tangential direction), and thus the concentration profile of the solute near the membrane surface on the liquid would be formed. The porosity, pore size, interval between pores, etc, could affect the solute concentration profile, and the effective mass transfer area could be between that of the whole membrane area and that of the total area of the pores. So, we set out to investigate this issue further, and explain how the effective mass transfer area changes in relation to the membrane porosity, the pore size and the absorption system.

In this work, five kinds of flat membranes with different porosity and pore size were chosen to carry out membrane absorption experiments with a

stagnant absorbent so that factors related to hydrodynamics, such as non-ideal flow and end-effects that other researchers have mentioned in connection with the hollow fiber membrane absorption process were eliminated. The experimental systems were pure CO₂-pure water and CO₂-NaOH solution. The influence of porosity and the pore size on the mass transfer behavior of the membrane absorption process has been investigated. Based on experimental results, the mechanism of how the porosity affected the mass transfer behavior of the membrane absorption process has also been discussed.

EXPERIMENT

In this experiment, pure CO₂ (gas phase) continuously flowed into the flat module during the absorption process, and the absorbent was either pure water or 0.1 M NaOH solution. Experimental setup is as shown in Fig. 1. Two vessels with 300 mm length, 150 mm width, and 25 mm height were connected together and the expanded polytetrafluoroethylene (ePTFE) flat membrane placed in between. The whole surface area of the membrane was 450 cm². Membrane structural parameters are listed in Table 1.

Before the experiment, pure CO₂ flowed into the vessel for about 30 min to purge the air out. When the experiment started, the vessel was filled up with 1000 ml absorbent as quickly as possible, and then both the outlet and the inlet of the liquid were plugged up by clip 11. The pressure of the gas phase was controlled at about 15 mm H₂O by seal 5 to prevent CO₂ from bubbling

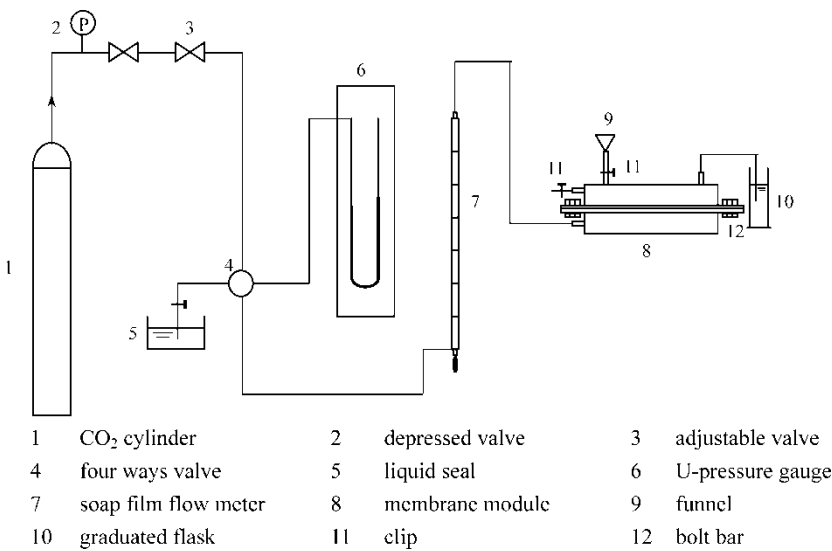


Figure 1. The experimental flow chart.

Table 1. Micro-structural parameters of membranes^a

	Mean pore size d (μm)	Surface porosity ε
1#	0.2	0.52
2#	0.2	0.89
3#	2	0.60
4#	2	0.85
5#	2	0.90

^aThe flat membranes were manufactured by the Military Center of the Quartermaster Research Institute of the General Logistics Department of PLA. The parameter of porosity was determined by wet and dry flow method.

through the liquid phase. The absorbed CO_2 flux was measured by a soap film flow meter. All the experiments were carried out at 20°C. As CO_2 was being absorbed, the pressure on the gas side began to decrease, and CO_2 continued to flow from the gas cylinder and passed through a flow meter 7 into the absorber to maintain the pressure balance. During the experiment, there was no outlet for both the gas and the absorbent though there was a continuous gas feed into the module (Fig. 1). This situation then means that the absorption process was at an unsteady state because the concentration of CO_2 in the liquid was increasing with time, bringing about reduced driving force. The soap film passed through the graduations which were noted as V_1, V_2, \dots, V_j with the accumulative time intervals recorded as t_1, t_2, \dots, t_j respectively. So, the CO_2 absorption rate from time t_{j-1} to t_j could then be calculated by Eq. (1) and the corresponding time by Eq. (2).

$$N(t_i) = \frac{V_j - V_{j-1}}{t_j - t_{j-1}} \quad (1)$$

$$t_i = t_{j-1} + \frac{t_j - t_{j-1}}{2} \quad (2)$$

where V_i is the absorbed CO_2 volume measured by soap film flowmeter.

RESULTS AND DISCUSSION

According to the *resistance-in-series* model, the mass transfer resistance was simply the arithmetic sum of the gas phase resistance, the liquid phase resistance, and the membrane phase resistance. In order to simplify the whole problem and distinguish which factors played the most important role for this experimental absorption process, pure gas was used to characterize the mass transfer resistance in the liquid phase. Since pure CO_2 was used, the gas phase resistance could be ignored. Due to the hydrophobicity of the

membrane, pure CO_2 filled in the membrane pores, and during the absorption process, the membrane resistance was just the resistance to gas diffusion through the gas itself in the micro-pores of the membrane. The membrane pore size ranged from $0.2 \mu\text{m}$ to $2 \mu\text{m}$, while the molecular mean free path of CO_2 at experimental conditions was about 100 nm (14), which is much smaller than that of the membrane pore size, justifying the Poiseuille flow through the membrane pores. If the gas diffusion rate is very small, the gas diffusion resistance in the membrane is very small too (14). So, the dominating mass transfer resistance in the membrane absorption process would be the diffusion resistance in the static liquid phase. The details would be further discussed later.

The Influence of Porosity on Membrane Absorption Process when the Mean Pore Size was Relatively Small

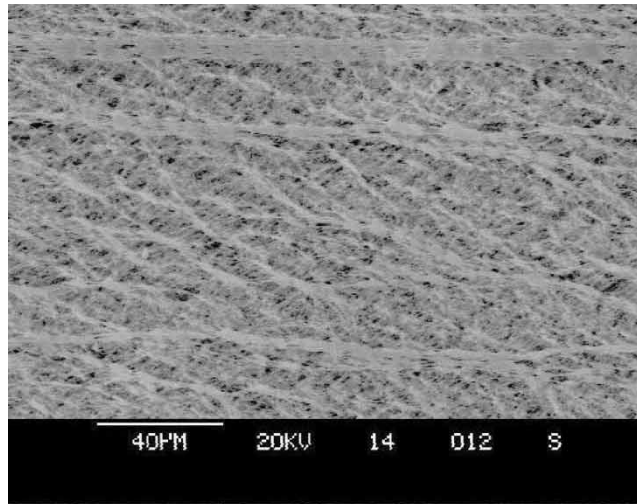
From Table 1, the pore size of 1# and 2# membranes was $0.2 \mu\text{m}$, which was smaller than that of 3#, 4# and 5# membranes. Figure 2 is the SEM photograph of 1# and 2# membranes. It is clear from this figure that the porosity of 2# membrane was bigger than that of 1# membrane. The absorption rates of CO_2 and their variation with time using 1# and 2# membrane were measured and the experimental results are shown in Fig. 3.

As Fig. 3(a) shows, when pure water was used as an absorbent, the absorption rate of 1# and 2# membranes varied with time and the trend was similar. In general, CO_2 absorption process in pure water is a physical absorption process, and the mass transfer process is relatively slow compared to CO_2/NaOH solution absorption process. So, for this kind of slow mass transfer system, the porosity of the membrane had a negligible influence on the membrane absorption process when the membrane mean pore size was relatively small.

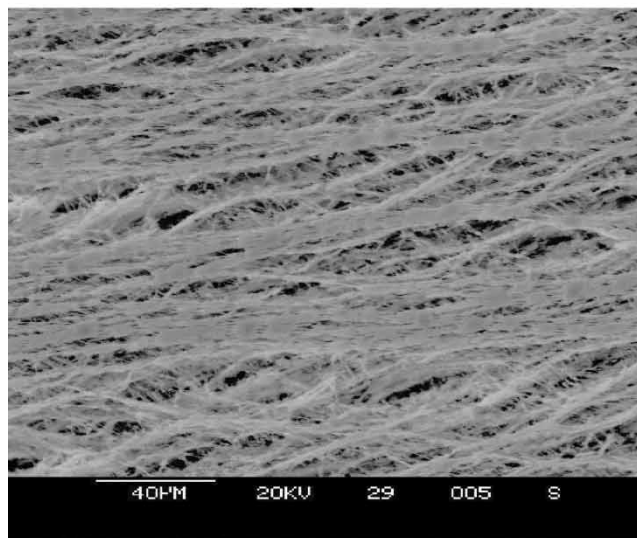
However, when 0.1 M NaOH solution was used as absorbent, the absorption rate of 2# membrane was higher than that of 1# membrane as Fig. 3(b) shows. Further, the absorption rate with its variation with time was different for 1# and 2# membranes. The process of CO_2 absorption in 0.1 M NaOH solution is enhanced by a chemical reaction, and so the mass transfer is relatively rapid. For a rapid mass transfer system, the influence of membrane porosity on the membrane absorption was even more serious when the mean pore size of membrane was small. In this case, the absorption rate was higher for higher membrane porosity.

The Influence of Porosity on Membrane Absorption Process when the Mean Pore Size was Relatively Big

As shown in Table 1, the pore size of 3#, 4# and 5# membranes was $2.0 \mu\text{m}$, which was bigger than that of 1# and 2# membranes. Figure 4 shows the SEM



(a) 1# membrane



(b) 2# membrane

Figure 2. The SEM photos of 1# and 2# membrane, (a) for 1# membrane, (b) for 2# membrane.

photographs of 3#, 4# and 5# membranes. The porosity of 3#, 4#, and 5# membranes was 0.60, 0.85, and 0.90 respectively. The absorption rates of CO_2 and their variation with time for 3#, 4#, and 5# membranes were measured. The experimental results are shown in Fig. 5.

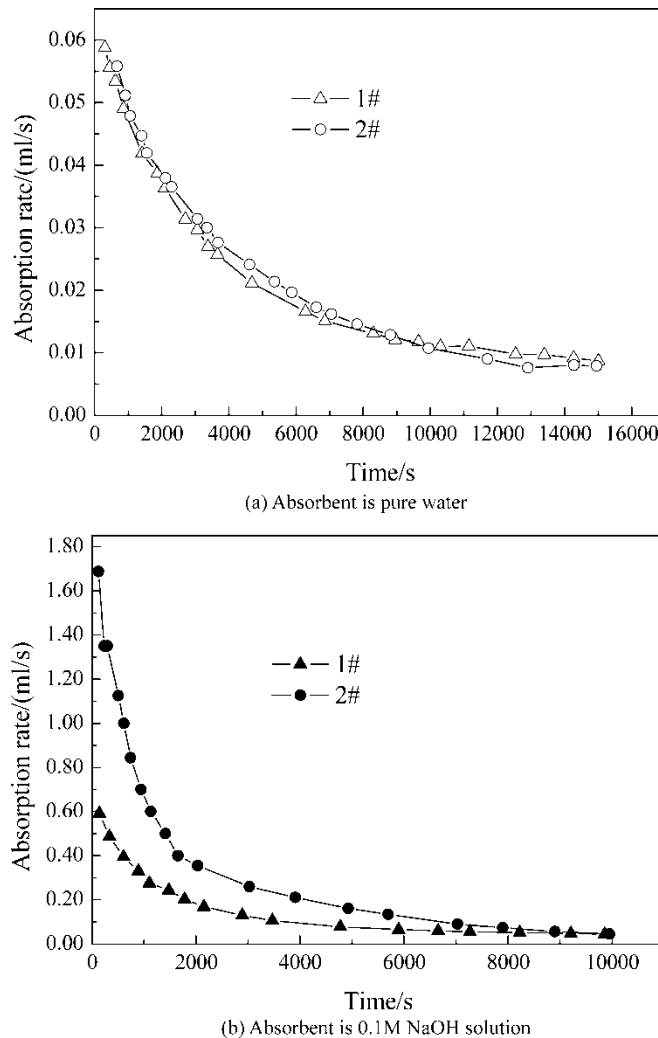


Figure 3. The absorption rate vs. time, when using 1# and 2# membrane (a) for the CO_2 -pure water system, (b) for CO_2 -0.1 M NaOH solution system.

As Fig. 5(a) shows, when pure water was used as an absorbent, the absorption rate of 3#, 4#, and 5# membranes varied with time in a similar fashion, just like the absorption rates for 1# and 2# membranes. However, in CO_2 /NaOH solution system, as shown in Fig. 5(b), it is obvious that the absorption rate increased with the increasing membrane porosity for 3#, 4#, and 5# membranes, but its variation with time was different, though the difference was not much compared to that for 1# and 2# membranes when 0.1 M NaOH solution was used as an absorbent (Fig. 3(b)).

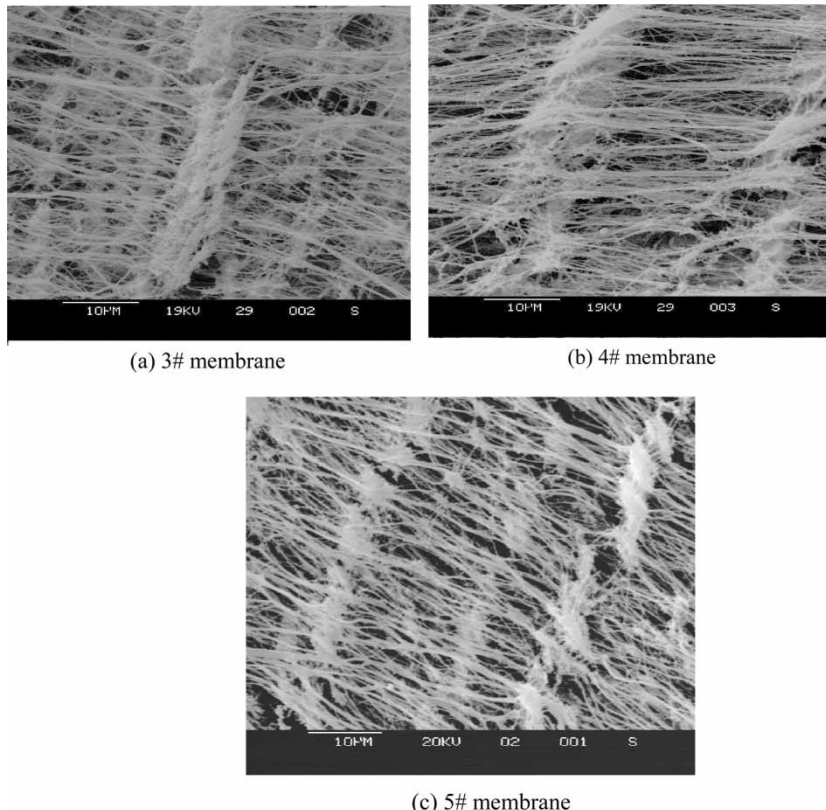


Figure 4. The SEM photos of 3#, 4#, and 5# membrane, (a) for 3# membrane, (b) for 4# membrane, (c) for 5# membrane.

Generally then, when the pore size of the membrane was bigger, for a rapid mass transfer system, the membrane porosity did have an effect on the mass transfer in the membrane absorption process, and the absorption rate also increased with increasing membrane porosity. At the same time, from Fig. 3(b) and Fig. 5(b), it could also be found that when the membrane pore size was smaller, the influence of the porosity on membrane absorption process was even more serious.

As a summary, according to the analysis above, it is known that for a slow mass transfer system, such as the physical absorption process, the membrane porosity had almost no influence on the membrane absorption process. However, for a rapid mass transfer system, such as chemical absorption, the membrane porosity did have influence on the membrane absorption process and the effect was even more serious when the pore size of the membrane was small.

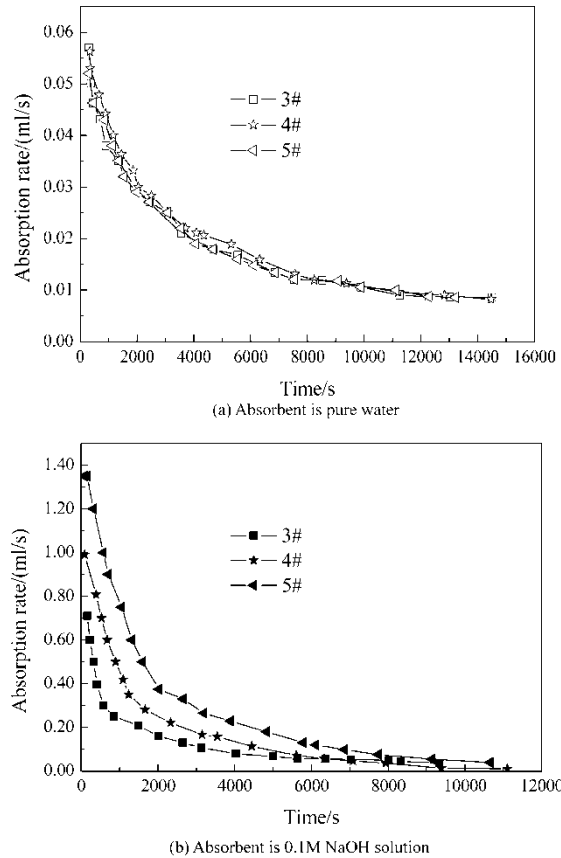


Figure 5. The absorption rate vs. time, when using 3#, 4#, and 5# membrane, (a) for the CO₂-pure water system, (b) for CO₂-0.1 M NaOH solution system.

The Mechanism of the Influence of Porosity on the Membrane Absorption Process

The Mathematical Model of the Overall Mass Transfer Coefficient

In an unsteady state membrane absorption process, the mass equilibrium of CO₂ on the liquid side yields:

$$\ln \left(\frac{N^* - \sum_{i=1}^n (N(t_i) \cdot \Delta t_i)}{N^*} \right) = - \frac{K_L A}{V} \cdot t_n \quad (3a)$$

$$\Delta t_i = t_n - t_{n-1} \quad (3b)$$

$$N^* = PHV \cdot RT/P = HVRT \quad (3c)$$

where A is membrane area, ($A = 0.045 \text{ m}^2$), H is *Henry's* coefficient of CO_2 in liquid, P is the gas pressure, R is the gas constant ($R = 8.314 \text{ Pa.m}^3/(\text{mol K})$), T is the experimental temperature (in this study, $T = 293.15 \text{ K}$), V is the volume of absorbent (in this study, $V = 1000 \text{ ml}$), and K_L is the overall mass transfer coefficient based on the liquid phase. The overall mass transfer coefficient could then be determined from a semilog plot of the flux rate versus time. The typical figure showing the plot based on Eq. 3 is shown in Appendix A.

As the CO_2 absorption process of this work was an unsteady state process, the overall mass transfer coefficient was rapidly reducing with time in the initial stage of the process. This initial stage was the most important part of the equilibrium CO_2 absorption flux as shown in Fig. 3 and Fig. 5. Since the mean overall mass transfer coefficient of the whole process time could not accurately characterize the process due to significant reduction in the driving force, the mass transfer behavior during the first 20 minutes should be taken into account in this work. Unfortunately, the absorption flux at the beginning of the experiment could not be measured accurately, because it needed at least 3–5 minutes to form a stable gas-liquid interface after the absorbent was fed into the module. So, the absorption process during 5–20 minutes has been considered in this paper.

The membrane resistance was calculated by Eq. (4), basing on the theory of Poiseuille flow (14).

$$\frac{1}{k_m} = \frac{8\mu L \tau_m}{\bar{P} \bar{r}^2} \quad (4)$$

where L is the membrane thickness, \bar{r} is the mean radius of membrane pores, \bar{P} is the mean pressure on the gas side, μ is viscosity of CO_2 , and the value is $1.37 \times 10^{-7} \text{ Pas}$ at 20°C and 101325 Pa . τ_m is the tortuosity of the membranes and is generally taken to be 2 (3, 5, 8).

Equation (3) was used to calculate the overall mass transfer coefficient for different membranes, using either pure water or 0.1 M NaOH solution as absorbent. The overall mass transfer coefficient vs. membrane porosity is shown in Fig. 6. From Fig. 6, it can be found that the membrane porosity had a insignificant effect on the overall mass transfer coefficient in pure water CO_2 absorption process. However, when 0.1 M NaOH solution was used as absorbent, the overall mass transfer coefficient increased with increasing membrane porosity.

Equation (3) and Eq. (4) were used to calculate the overall mass transfer resistance, $1/K_L$ and the mass transfer resistance of the membrane, $1/k_m$ respectively for each membrane. The results are shown in Table 2. It could be found that the membrane resistance was quite small compared to the overall mass transfer resistance for each membrane, and the contribution of the membrane resistance in the overall mass transfer resistance was $\leq 7.37\%$, and could be ignored in this study.

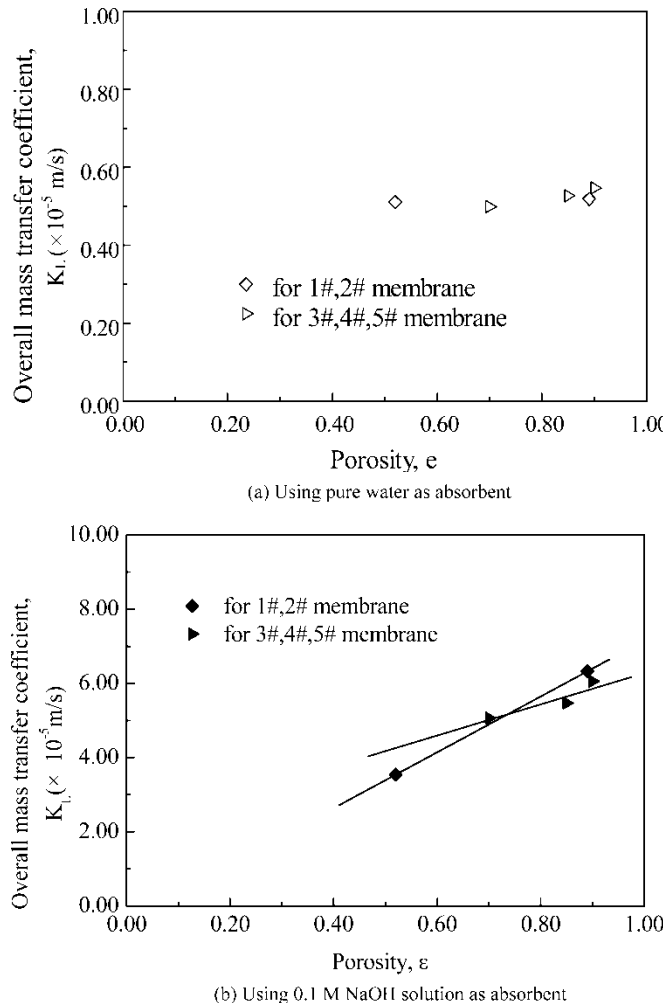


Figure 6. Overall mass transfer coefficient vs. porosity, (a) for the CO_2 -pure water system, (b) for CO_2 -0.1 M NaOH solution system.

Modeling Calculation and Analysis

According to the analysis above, the overall mass transfer resistance in the membrane absorption process was controlled by diffusion of CO_2 on the liquid side. As shown in Fig. 7, when CO_2 transfers through the membrane pores, the concentration profile of CO_2 would be formed, and would approach the concentration in the bulk liquid at point “ l ”, from the surface of the membrane. In other words, the distance “ l ” is just equal to the thickness of the liquid boundary layer through which the solute had to

Table 2. Comparison between the overall mass transfer resistance and membrane resistance for each membrane

Membrane resistance, $1/k_m$ (s/m)	Overall mass transfer resistance when using pure water as absorbent, $1/K_L$ (10^5 s/m)	Overall mass transfer resistance when using 0.1 M NaOH solution as absorbent, $1/K_L$ (10^5 s/m)
1#	0.015	1.98
2#	0.012	1.95
3#	0.00024	2.03
4#	0.00013	1.92
5#	0.00021	1.85

diffuse before reaching the bulk liquid. According to the analysis of the membrane absorption process, there were transfer zones and non-transfer zones near the membrane surface on the liquid side as shown in Fig. 7 and therefore the mass transfer area must be somewhere in between the total area of the micro pores and the whole membrane surface area.

The diffusion distance “ l ” could be calculated based on the following assumptions:

1. Ideal gas behavior and *Henry*’s law are applicable,
2. CO_2 does not accumulate in the “ l ” layer, and the reaction with OH^- only takes place at point “ l ” from the membrane or in the bulk liquid,
3. The concentration of OH^- in the bulk liquid remains constant (because the volume of the absorbent is excessive),
4. The velocity of CO_2 moving through the “ l ” layer was v_s .

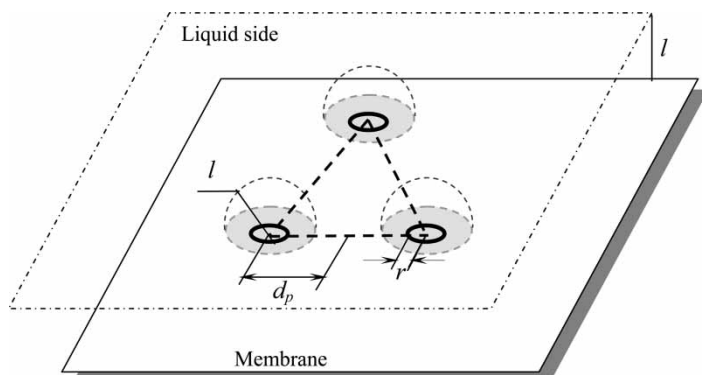


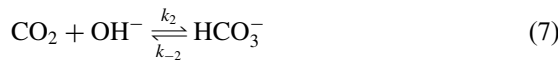
Figure 7. The schematic of CO_2 diffusion in liquid side near the membrane surface after transferring through the membrane pores.

So, the time t_s that CO_2 concentration profile transfer through the “ l ” layer could be calculated by the following equation

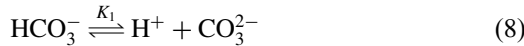
$$t_s = l/v_s \quad (5)$$

When CO_2 moved through the “ l ” layer with the apparent velocity as v_s , the apparent velocity of the liquid was v_s in the opposite direction. So, the flux of CO_2 through the “ l ” layer could be calculated as $v_s \cdot A \cdot \Delta C$ at time t . At the same time, the flux of CO_2 through the “ l ” layer could also be calculated as $K_L \cdot A \cdot \Delta C$. So, the value of v_s would be equal to the value of K_L .

When CO_2 is absorbed in pure water or 0.1 M NaOH solution, there is a reaction between CO_2 and OH^- , because the absorbent is in excess. The only difference is that when pure water or 0.1 M NaOH solution is used as absorbent, the value of $[\text{OH}^-]$ is 10^{-7} mol/l or 0.1 mol/l respectively. The rate controlling reactions are given by (15).



where k_1 , k_{-1} , k_2 , and k_{-2} are the reaction constants respectively. The following two more reactions are involved and they are very fast reactions so that they are assumed to be at equilibrium:



where K_1 and K_2 are the equilibrium constants.

According to assumptions (2) and (3), the depletion rate of CO_2 due to the reaction with OH^- ion in time t could be calculated as follows (15).

$$\frac{dC_{\text{CO}_2}}{dt} = -(k_1 + k_2[\text{OH}^-]) \times \left(C_{\text{CO}_2} - \frac{k_{-1}K_2}{k_1} \cdot \frac{1}{[\text{OH}^-]} \right) \quad (10)$$

Using Eq. (5), Eq. (10) can also be written as

$$\int_{C^*}^{C_b} \frac{dC_{\text{CO}_2}}{\left(C_{\text{CO}_2} - ((k_{-1}K_2)/k_1) \cdot (1/[\text{OH}^-]) \right)} = \int_0^{t_s} -(k_1 + k_2[\text{OH}^-]) dt \quad (11a)$$

$$t_s = l/v_s = l/K_L \quad (11b)$$

where C^* is the equilibrated concentration of CO_2 at the interface, C_b is the concentration of CO_2 in the bulk liquid, which could be calculated by integrating the absorbed CO_2 with time by Eq. (13).

Eq. (11) can be integrated to get the value of “*l*” as follows

$$l = \frac{K_L \times \ln \left(\frac{C^* - \frac{k_{-1}K_2}{k_1} \cdot \frac{1}{[\text{OH}^-]}}{C_b - \frac{k_{-1}K_2}{k_1} \cdot \frac{1}{[\text{OH}^-]}} \right)}{(k_1 + k_2[\text{OH}^-])} \quad (12)$$

$$C_b = \frac{\int N(t)dt}{V_{\text{absorbent}}} = \frac{\sum N(t) \cdot \Delta t}{V_{\text{absorbent}}} \quad (13)$$

According to the assumptions and Eq. (12), Eq. (13), the value of “*l*” was calculated and is shown in Table 4. The parameters used in the calculation are shown in Table 3.

As shown in Fig. 7, the pores on the membrane surface could be arranged as equilateral triangles since the number of pores is large, and the porosity can be expressed as follows (16) according to Fig. 7.

$$\varepsilon = \frac{(1/2)\pi r^2}{(\sqrt{3}/4)(2d_p)^2} \quad (14)$$

So, half the interval between pores could be calculated by Eq. (15). The calculated results are listed in Table 4, too.

$$d_p = \frac{1}{2} \sqrt{\frac{2\pi}{\sqrt{3} \cdot \varepsilon}} \cdot r \quad (15)$$

Analyzing the results in Table 4, when pure water was used as an absorbent, there was *l* > *d*_{*p*}, that means, when CO₂ diffused through the

Table 3. The parameters used in the calculation^a

Parameters	Value
The equilibrated concentration of CO ₂ in the interface, <i>C</i> _{CO₂} [*] mol/m ³ (17)	33.84 for pure water 83.84 for 0.1 M NaOH solution
The Henry's coefficient of CO ₂ in liquid, H, mol/(m ³ · Pa) (18)	3.34 × 10 ⁻⁴ for pure water, 8.27 × 10 ⁻⁴ for 0.1 M NaOH solution
Reaction rate constant, <i>k</i> ₁ , s ⁻¹ (19)	log <i>k</i> ₁ = 3.29.85 – 110.54 log <i>T</i> – (17265.40/ <i>T</i>), <i>T</i> : K
Reaction rate constant, <i>k</i> ₂ , dm ³ mol ⁻¹ s ⁻¹ (19)	log <i>k</i> ₂ = 13.653 – (289.5/ <i>T</i>), <i>T</i> : K
Equilibrium constant, <i>K</i> ₁ (19)	log <i>K</i> ₁ = (–3404.7/ <i>T</i>) + 14.843 – 0.03279 <i>T</i> , <i>T</i> : K
Equilibrium constant, <i>K</i> ₂ (19)	1 × 10 ⁻¹⁴

^aall parameters are calculated at 20°C and 101325 Pa.

Table 4. Comparing the pore interval with the layer “*l*” for pure water or 0.1 M NaOH solution absorption

Porosity	The layer “ <i>l</i> ” for pure water absorption (/ 10^{-7} m)	The layer “ <i>l</i> ” for 0.1 M NaOH solution absorption (/ 10^{-7} m)	The half interval of pores, d_p (/ 10^{-7} m)
	(/ 10^{-7} m)	(/ 10^{-7} m)	
1#	0.52	26.33	1.32
2#	0.89	25.12	0.97
3#	0.70	27.52	1.20
4#	0.85	26.14	1.45
5#	0.90	25.03	0.99

boundary layer and reached the bulk liquid in the normal direction, the distance that CO_2 diffused in the horizontal direction was larger than the distance between the membrane pores. So, at point “*l*” from the membrane surface, the concentration profile of the solute could cover the entire membrane surface (see in Fig. 8). In this case, the whole membrane surface area could be treated as the effective mass transfer area, and the porosity could not affect the membrane absorption process. Experimental results, which are shown in Fig. 3(a), Fig. 5(a) and Fig. 6(a), support this hypothesis.

When the 0.1 M NaOH solution was used as absorbent, from Table 4, it could be found that $l < d_p$, which means that the base of the orbicular fluid infinitesimals only covered a part of the membrane surface and there were a lot of “dead” areas in between the membrane pores (see in Fig. 9). In this case, the porosity has a serious impact on the membrane absorption process, as shown in Fig. 3(b), Fig. 5(b) and Fig. 6(b).

Prior to this study, many other authors concluded that the influence of membrane porosity on the membrane absorption process was only limited to the membrane phase resistance (3, 5, 8), and this resistance was calculated by Eq. (4). However as it has already been discussed above, the membrane porosity actually affected the concentration profile of CO_2 near the

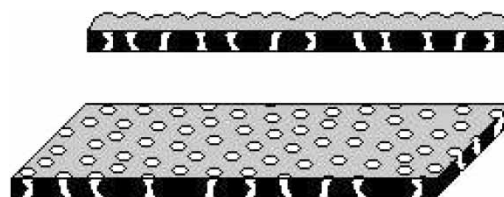


Figure 8. The schematic of the solute diffusing in the membrane surface of liquid side when $l > d_p$.

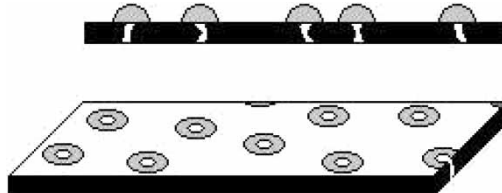


Figure 9. The schematic of the solute diffusing in the membrane surface of liquid side when $l < d_p$.

membrane surface on the liquid side, which led to a reduced mass transfer area, and a serious impact on the membrane absorption process.

CONCLUSIONS

Five kinds of flat membranes, with different pore size and porosity, were chosen to carry out the membrane-based CO_2 absorption experiment. The influence of porosity on mass transfer was investigated. These experimental results show that the porosity has little influence on the membrane absorption process when using pure water as absorbent. However, when using 0.1 M NaOH solution as absorbent, the influence of porosity on the membrane absorption process is complex. For a membrane with a relatively small pore size, the porosity affects the membrane absorption process significantly. In the case of using the membrane with a relatively big pore size, the porosity could affect the membrane absorption process but the influence could not be so serious.

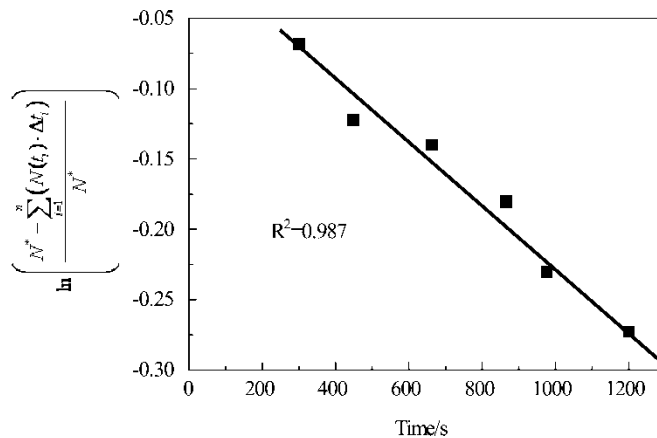


Figure 10. A typical figure showing the plot based on Eq. (3).

A theoretical analysis has shown that the porosity affects the concentration profile of CO_2 near the membrane surface on the liquid side, which led to the loss of the membrane mass transfer area, and then affect membrane absorption process. In a further study, the influence of porosity on the steady state membrane absorption process in a hollow fiber membrane module with both the gas mixture and liquid flowing would be considered.

APPENDIX A

A typical figure showing the plot based on Eq. (3) is shown in Fig. 10. From Fig. 10, the degree of linear correlation is good.

NOMENCLATURE

A	The membrane area (m^2)
C	The concentration of the solute (CO_2) in the liquid (mol/m^3)
C_b	The concentration of the solute (CO_2) in the bulk fluid (mol/m^3)
C^*	The equilibrated of the solute (CO_2) in the liquid by <i>Henry</i> law (mol/m^3)
d	The diameter of the pore (m)
d_p	The half interval between the pores (m)
D	The diffusion coefficient of the solute in the liquid (m^2/s)
P	The pressure in the gas side (pa)
H	The <i>Henry</i> coefficient of CO_2 in water ($\text{mol}/(\text{m}^3 \cdot \text{pa})$)
K_L	The overall mass transfer coefficient based on liquid phase (m/s)
K_1	The equilibrium constant of reaction ⁸ (mol/dm^3)
K_2	The equilibrium constant of reaction ⁹ (mol^2/dm^6)
k_m	The mass transfer coefficient of membrane (m/s)
k_1	The forward rate of constant of reaction ⁶ (s^{-1})
k_{-1}	The reverse rate of constant of reaction ⁶ ($\text{dm}/(\text{mol} \cdot \text{s})$)
k_2	The forward rate of constant of reaction ⁷ ($\text{dm}^3/(\text{mol} \cdot \text{s})$)
k_{-2}	The reverse rate of constant of reaction ⁷ (s^{-1})
l	The thickness of the imaginary stagnant film (m)
N	The absorption rate (ml/s)
R	The gas constant ($\text{Pa} \cdot \text{m}^3/(\text{mol} \cdot \text{K})$)
T	The experimental temperature (K)

Greek Letters

ε	The surface porosity in each cell of the membrane (-)
μ	The viscosity of CO_2 (Pas)
ν_s	The superficial transport velocity of CO_2 in "l" layer (m/s)

ACKNOWLEDGEMENTS

This work was supported by the National Natural Science Foundation of China (No. 20206002), the University Doctor of Science Foundation of China (No. 20020010004), the Beijing NOVA Program (H013610250112) and the Important Sci-Tech Research Program of the Ministry of Education of China (Important: 01025).

REFERENCES

1. Esato, K. and Eiseman, B. (1975) Experimental evaluation of Gore-Tex membrane oxygenator. *J. Thorac. Cardiovascular Surg.*, 69: 690–701.
2. Yang, M.C. and Cussler, E.L. (1986) Designing hollow fiber contactors. *AIChE J.*, 32: 1910–1923.
3. Zhang, Qi. and Cussler, E.L. (1985) Microporous hollow fibers for gas absorption. I. Mass transfer in the liquid. *J. Membr. Sci.*, 23 (2): 321–332.
4. Ogundiran, O.S., LeBlanc, S.E., and Varanasi, S. (1989) Membrane contactors for SO₂ removal from flue gases. In *The Pittsburgh Coal Conference*; Pittsburgh, PA.
5. Susum, Nii., Kakeuchi, H., and Takahashi, K. (1992) Removal of CO₂ by gas absorption across a polymeric membrane. *J. Chem. Eng. Jpn*, 25 (1): 67–72.
6. Wang, K.L. and Cussler, E.L. (1993) Baffled membrane modules made with hollow fiber fabric. *J. Membr. Sci.*, 85 (2): 279–281.
7. Xu, G.-W., Zhang, C.-F., Qin, S.-J., Gao, W.-H., and Liu, H.-B. (1998) Gas-liquid equilibrium in CO₂-MDEA-H₂O system and the effect of piperazine on it. *Ind. Eng. Chem. Res.*, 37: 1473–1488.
8. Bhave, R.R. and Sirkar, K.K. (1986) Gas permeation and separation by aqueous membranes immobilized across the whole thickness or in a thin section of hydrophobic microporous celyard films. *J. Membr. Sci.*, 27 (1): 41–59.
9. Gao, J., Zhang, W., Chen, S., and Zhang, Z. (2005) The influence of chemical reaction on mass transfer behavior in the membrane absorption process. *Sep. Sci. & Tech.*, 40 (6): 1227–1246.
10. Kim, Y.-S. and Yang, S.-M. (2000) Absorption of carbon dioxide through hollow fiber membranes using various aqueous absorbents. *Sep. Purif. & Tech.*, 21: 101–109.
11. Baudot, A., Flory, J., and Smorenburg, H.E. (2001) Liquid-liquid extraction of aroma compounds with hollow fiber contactor. *AIChE J.*, 47 (8): 1780–1795.
12. Karoor, S. and Sirkar, K.K. (1993) Gas absorption studies in microporous hollow fiber membrane modules. *Ind. Eng. Chem. Res.*, 32: 674–683.
13. Kreulen, B.H., Smolders, C.A., Versteeg, G.T., and van Swaaij, W.P.M. (1993) Microporous hollow fiber membrane modules as gas – liquid contactors. Part I. Physical mass transfer processes. A specific application: Mass transfer in highly viscous liquids. *J. Membr. Sci.*, 78 (1): 197–216.
14. Kast, W. and Hohenhanner, C.-R. (2000) Mass transfer within the gas-phase of porous media. *Int. J. Heat Mass Transfer*, 43: 807–813.
15. Suchdeo, S.R. and Schultz, J. (1974) The permeability of gases through reacting solutions: the carbon dioxide – bicarbonate membrane system. *Chem. Eng. Sci.*, 29: 13–21.
16. Chen, V. and Hlavacek, M. (1994) Applications of Voronoi tessellation for modeling randomly packed hollow fiber bundles. *AIChE J.*, 40: 606–617.

17. Brutsaert and Wilfried and Jirka Ggerhard, H. (1984) *Gas Transfer at Water Surface*; D. Reicel Publishing Company: Boston, MA.
18. Zhang, C.F. (1985) *Gas Liquid Reaction and Reactor*; Chemical Industry Press of China: Beijing.
19. Dankwerts, P.V. and Sharma, M.M. (1966) The absorption of carbon dioxide into solutions of alkalis and amines (with some notes on hydrogen sulfide and carbonyl sulfide). *Chem. Eng.*, 244–255.